Transition between Light- and Heavy-Ion Elastic Scattering

R. M. DeVries
Nuclear Structure Research Laboratory, University of Rochester, Rochester, New York 14627

and

D. A. Goldberg
Department of Physics and Astronomy, University of Maryland, College Park, Maryland 20743

and

J. W. Watson
Department of Physics, University of Manitoba, Winnepeg, Manitoba R3T 2N2, Canada and Crocker Nuclear Laboratory, University of California, Davis, California 94720

and

M. S. Zisman
Lawrence Berkeley Laboratory, Berkeley, California 94720

and

J. G. Cramer
Nuclear Physics Laboratory, University of Washington, Seattle, Washington 98195
(Received 24 June 1977)

We have measured the elastic scattering from ^{28}Si of 135.1-MeV ^{6}Li and 186-MeV ^{12}C ions. The shapes of the angular distributions and the resultant optical-model analyses indicate that ^{6}Li scattering is quite similar to that of light ions, while ^{12}C ions behave like heavier ions. Thus there appears to be a pronounced and quite rapid transition of scattering characteristics with projectile mass.

Recently we showed[1] that high-energy ($E_i = 215$ MeV) ^{16}O + ^{28}Si elastic scattering exhibits angular distributions and resultant optical-model parameters which are quite different from those observed for light ions. In particular, high-energy light-ion angular distributions exhibit at angles beyond the diffraction oscillations a structureless falloff characteristic of a nuclear rainbow.[2] These rainbow data not only allow the determination of the strength of the real part of the potential but also indicate that light-ion optical potentials have a central imaginary well depth $\frac{1}{3}-\frac{1}{6}$ of the real depth. Furthermore, both the real and imaginary depths of light-ion potentials are energy dependent.[3] In contrast, our results for ^{16}O scattering[1] indicated (a) no evidence of rainbow scattering effects, (b) $W/V \geq 1$ in the nuclear surface, and (c) good fits with an energy-independent potential.

The purpose of the present study was to explore what happens with projectiles of masses intermediate to light (d, ^{3}He, α) and heavy (^{16}O) ions. Data were taken using ^{6}Li^{3+} (135.1 MeV) and ^{12}C^{4+} (186.4 MeV) beams from the Lawrence Berkeley Laboratory (LBL) 88-in. cyclotron. Most of the data were taken using the counter system described in Ref. 1; a portion of the ^{6}Li data was acquired using the LBL quadrupole-sextupole-dipole spectrometer. An additional experimental refinement consisted of correcting for the zero-angle drift in the beam by monitoring the ground-state/2^{+}(1.78 MeV) intensity ratio as recorded by a counter placed at a fixed angle. The error bars in the data include the $\pm 0.1°$ uncertainty associated with these corrections. Existing ^{6}Li data at 13 MeV[4] and ^{12}C data at 24 MeV[5] and 49.3 MeV[6] are shown in Fig. 1 along with the new data. The difference in the shapes of the two high-energy data sets is striking. Specifically, ^{6}Li + ^{28}Si displays at large angles the characteristic structureless falloff of nuclear rainbow scattering typical of light-ion scattering, while ^{12}C + ^{28}Si displays instead a diffractive, oscillatory angular distribution very similar to ^{16}O scattering.

Optical-model analyses of the data sets yield equally distinctive results. The ^{12}C data have been analyzed in a manner similar to that employed with the ^{16}O data[1]; i.e., searches were performed (with the code GENOA[7]) on the 24- and 186.4-MeV data simultaneously. The potentials

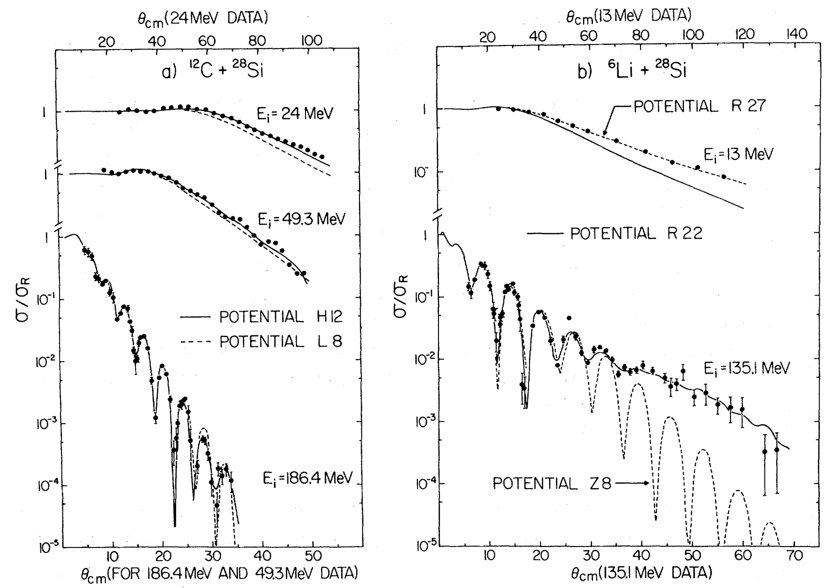

FIG. 1. Elastic scattering of ^{12}C and ^{6}Li from ^{28}Si. Note that the high-energy ^{12}C scattering is similar to ^{16}O scattering (Ref. 1) while the high-energy ^{6}Li data is similar to light-ion data (Ref. 2).

which result from such an energy-independent assumption provide a convenient characterization of the data and permit comparison with ^{16}O potentials derived in an identical manner. Two real well depths were chosen ($V_0 = 10$ and 100 MeV) while all other parameters were varied, resulting in the parameters shown in Table I and fits displayed in Fig. 1(a). The $V_0 = 10$-MeV potential (H12) yields excellent fits with parameters very similar to those obtained from the ^{16}O analysis[1]; the $V_0 = 100$ MeV potential (L8) fails to give comparably good fits to the data, also in accord with our ^{16}O results. One slight difference between ^{12}C and ^{16}O scattering is that a somewhat better fit to the low-energy (24 MeV) ^{12}C data (χ^2/F improving by a factor of 2) can be obtained by fitting those data separately; no such effect was observed in analyzing the ^{16}O data.

The 10-MeV potential (H12) also predicts correctly the overall behavior of the data of Kohno *et al.*[6] at the intermediate energy of 49.3 MeV, although it fails to reproduce the oscillations appearing at larger angles [see Fig. 1(a)]. However, here again the situation parallels the ^{16}O case where similar structure is observed which cannot be fitted by any potential resembling those capable of fitting either the high- or low-energy data.[8]

In contrast, the optical-model analysis of the ^{6}Li data yields quite different results. As might be expected from the presence of the nuclear rainbow, a reasonable fit to the 135.1-MeV data cannot be obtained with a well depth shallower than ~100 MeV; as can be seen from Fig. 1(b), the "best-fit" 10-MeV potential (Z8), which is quite similar to E18 and H12, fails utterly to fit the data in the rainbow region. However, a potential with $V_0 = 150$ MeV (R22) or greater yields an excellent fit to the complete angular distribution. Moreover, it is not possible to fit both the 13-MeV and 135.1-MeV data sets with a single poten-

TABLE I. ^{12}C + ^{28}Si Woods-Saxon optical-model potentials.

Set	V_0 (MeV)	$r_0^{\,a}$ (fm)	a_0 (fm)	W_0 (MeV)	$r_I^{\,a}$ (fm)	a_I (fm)	χ^2/F (186.4-MeV data)
	Parameters						
H12	10	1.32	0.617	30.3	1.16	0.609	2.3
L8	100	0.868	0.838	42.7	1.08	0.743	5.1

$^{a}R = r(12^{1/3} + 28^{1/2})$.

TABLE II. $^{6}Li + ^{28}Si$ Woods-Saxon optical-model potentials.

Set	V_0 (MeV)	r_0[a] (fm)	a_0 (fm)	W_0 (MeV)	r_I[a] (fm)	a_I (fm)	χ^2/F (135.1-MeV data)	Volume integral (MeV fm^3)	Θ_R[b] (deg)
Z8	10	1.34	0.809	82.1	0.955	0.727	12	478	−11
V27	100	0.828	0.833	53.2	0.841	1.10	3.0	1384	−56
R22	150	0.727	0.877	44.4	0.904	1.06	2.6	1587	−72
R27	150	0.682	0.828	38.8	1.02	0.889	28	1318	−71
Q5	200	0.679	0.871	66.1	0.795	1.08	2.8	1809	−95
M4	250	0.636	0.872	54.7	0.848	1.07	2.7	1964	−112

[a]$R = r(28^{1/3} + 6^{1/3})$, i.e., the heavy-ion convention; more reasonable values of r are obtained with the light-ion convention $R = r(28^{1/3})$.

[b]Nuclear rainbow angle (Ref. 2).

tial. The best simultaneous fit to the 135.1-MeV and 13-MeV data sets with $V_0 = 150$ MeV yields a χ^2/F for the 13-MeV data which is a factor of 15 greater than that of the best fit to those low-energy data along (potential R27). We have also applied the potentials of Table II to intermediate-energy data[9] with the result that no set of energy-independent ^{6}Li optical parameters could be found. Therefore, in terms of both energy dependence and well strength, the ^{6}Li potential much more nearly resembles those for light ions than those for ^{12}C and ^{16}O.

On the other hand, analysis of the 135-MeV data indicates differences between ^{6}Li scattering and that of the lighter ions. Despite the presence of a nuclear rainbow, we are unable to determine unambiguously the central well depth of the real potential (see Table II). Possibly this is simply due to the fact that although the data clearly indicate the presence of a rainbow, the analysis does not conclusively indicate that the data extend beyond the actual rainbow angle, the condition required for unambiguous determination of the potential in light-ion scattering.[2] However, it may be that the more strongly absorbing nature of the scattering, manifested by the large values of the imaginary diffuseness shown in Table II (they are almost double the values observed for α particles), is beginning to reduce the sensitivity of the scattering to the real part of the potential. Other contrasts with α-scattering results, namely the breadth of the continuous ambiguity, as observed in the analysis of the forward-angle diffraction scattering,[10] the fact that inclusion of the large-angle data appears almost to obliterate the distinction between the various so-called optical-model families, and the fact that all potentials give virtually identical predictions at forward angles, give credence to this interpretation.

In summarizing our results, we have determined that there is a pronounced transition from light-ion to heavy-ion scattering, the most striking aspect of which is the rapidity with which it occurs. By $A = 6$ it appears to have only begun; by $A = 12$ it appears to be complete. While energy dependence of the potentials has been predicted[11] to decrease with increasing projectile mass (consistent with our data), we are unaware of any theoretical treatment which explains the abrupt change of the potential from moderately absorptive and refractive to very strongly absorbing and diffracting. Clearly also, further high-energy experiments in the $A = 7$ to 11 mass region are needed to elucidate the nature of this transition.

We would like to thank N. Rust for his help with the analysis of the data and the Kansas State group for the use of their data prior to publication. We would like to thank C. F. Maguire for his assistance with some of the ^{6}Li measurements. Finally, we wish to acknowledge the assistance of the staff and operating personnel at the LBL 88-in. cyclotron which made possible the success of the experiments reported here.

This work was supported in part by the National Science Foundation, by the U. S. Energy Research and Development Administration, and by the National Research Council.

[1]J. G. Cramer, R. M. DeVries, D. A. Goldberg, M. S. Zisman, and C. F. Maguire, Phys. Rev. C 14, 2158 (1976).

[2]D. A. Goldberg and S. M. Smith, Phys. Rev. Lett. 29, 500 (1975); D. A. Goldberg, S. M. Smith, and G. F. Burdzik, Phys. Rev. C 10, 1367 (1974).

[3]P. P. Singh, P. Schwandt, and G. C. Yang, Phys. Lett. 59B, 113 (1975); S. M. Smith *et al.*, Nucl. Phys.

A207, 273 (1973); L. W. Put and A. M. J. Paans, Phys. Lett. 49B, 266 (1974).
[4]J. E. Poling, E. Norbeck, and R. R. Carlson, Phys. Rev. C 13, 648 (1976).
[5]J. S. Eck, T. J. Gray, and R. K. Gardner, Bull. Am. Phys. Soc. 22, 563 (1977); J. S. Eck, private communication.
[6]I. Kohno, S. Nakajima, T. Tonuma, and M. Odera, J. Phys. Soc. Jpn. 30, 910 (1971).
[7]F. Perey, unpublished.
[8]P. Braun-Munzinger *et al.* [Phys. Rev. Lett. 38, 944 (1977)] have been able to fit such data but only by employing direct modification of the S-matrix elements.
[9]K. Bethge, C. M. Fou, and R. W. Zurmühle, Nucl. Phys. A123, 521 (1969); R. M. DeVries, D. S. Shapira, N. Anantaraman, R. Cherry, M. R. Clover, and H. E. Gove, to be published.
[10]J. G. Cramer, R. M. DeVries, D. A. Goldberg, M. S. Zisman, and C. F. Maguire, Bull. Am. Phys. Soc. 21, 554 (1976).
[11]D. F. Jackson and R. C. Johnson, Phys. Lett. 49B, 249 (1974).

Nonlinear Evolution of Collisionless and Semicollisional Tearing Modes

J. F. Drake and Y. C. Lee
Center for Plasma Physics and Fusion Engineering, University of California, Los Angeles, California 90024
(Received 25 January 1977)

The evolution of a single tearing mode is investigated. The "collisionless" and "collisional" tearing modes nonlinearly evolve into the "semicollisional" regime where the dynamics of the "singular layer" are dominated by electron diffusion along the perturbed magnetic surfaces. The "semicollisional" mode grows algebraically in the nonlinear phase as in the "collisional" calculation of Rutherford.

Tearing instabilities are believed to have an important role in both the overall stability and energy confinement of tokamak discharges. The $m=2$ tearing mode (where m is the poloidal mode number) is experimentally found[1] to precede the "disruptive instability", although the role of this mode in the disruption is still unknown. Higher-order tearing modes, though smaller in amplitude, may break up the magnetic surfaces in tokamaks, resulting in enhanced particle and energy transport.[2,3] It is important, therefore, to develop an understanding of the nonlinear evolution of these instabilities. Previous nonlinear theories have been largely based on the collisional magnetohydrodynamics (MHD) equations. We have recently shown,[4] however, that the usual linear stability analysis which results from these equations[5] is not adequate to describe present high-temperature discharges. Evidently, the nonlinear treatment of these instabilities[6,7] must be modified accordingly.

For simplicity, we consider a model in which a current slab J_{z0} of width a in the x direction and uniform in the y-z plane flows along an externally produced B_{z0} field. A self-consistent field $B_{y0}(x)$ is produced which is given by $B_{y0}(x) \simeq B_{z0}x/l_s$ near $x=0$, with $l_s = B_{z0}(\partial B_{y0}/\partial x)^{-1}$ the shear length of the field. Density and temperature gradients are neglected. The magnetic energy in the field B_{y0} drives the tearing instability and, for a wave number k in the y direction, produces the magnetic islands shown in Fig. 1. The magnetic perturbations are represented by $\tilde{\vec{B}} = \nabla \times \tilde{A}_z \hat{e}_z$, where $\tilde{A}_z$ is the vector potential. The magnetic energy released is dissipated by an induced electric field $\tilde{E}_z = -c^{-1}\partial \tilde{A}_z/\partial t$ which accelerates electrons in a narrow region $|x| < \Delta \ll a$, where $\vec{k}\cdot\vec{B}_0 \approx 0$ ("singular layer"). The current J_z is filamented along the y direction by this induced field so

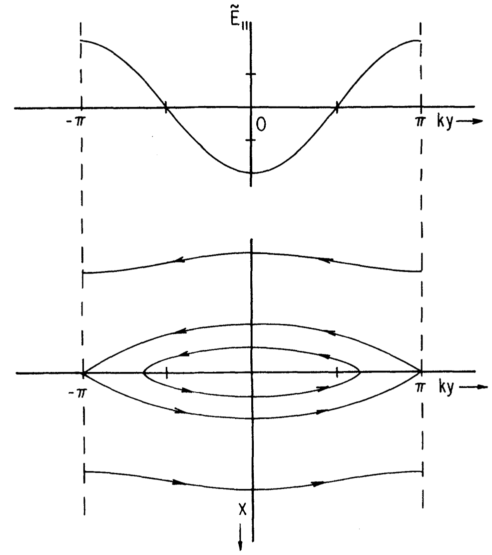

FIG. 1. The variation of $\tilde{E}_{\parallel}$ with y and the magnetic-field configuration around the tearing layer are shown. We assume $B_z \gg |B_y|, |B_x|$.